RESEARCH ARTICLE

Higher Neural Functions and Behavior

processings of moving and static objects (13), the average position of a moving object over a certain time (14), postdictive assignments of the post-flash positions to the moment of flashes (15), and predictive assignments of perceived positions (8, 16). Despite the contradictions among the various psychophysical mechanisms, it appears to be gradually realized that none of the mechanisms could singly interpret all of the rich FLE phenomena (4, 6, 17). One common conception of most mechanisms is that motion perception intricately links with position perception (9, 18). However, it is unclear whether modulation of neural activation in cortical areas selectively processing motion could affect motion-induced position mislocalization. Although one study has found the reduced FLE due to neural disruption in area MTþ (4), the neural processes underlying the causal contribution of area MTþ to the FLE are poorly understood.

Area MTþ plays a central role in visual motion processing (19, 20). Neuroimaging studies have found motion perception deficits in patients with brain damage localized to MTþ (21, 22). And transcranial magnetic stimulation (TMS) studies of MTþ observed visual motion perception impairment (22–25). Interestingly, MTþ shows preferential motion processing and attention to motion in the contralateral visual field (21, 22, 26), although it could potentially integrate motion in the left and right hemifields (25, 27). The motion processing pref-

Stimulus presentation.

Under the environment of MATLAB (2020a, The MathWorks, Natick, MA), we used Psychtoolbox-3 to present all visual stimuli on a color monitor [27-in. (68.58 cm) DP with a frame rate of 100 Hz] controlled by a personal computer (39, 40).

Stimuli and the flash-lag task.

Stimuli consisted of a white fixation cross, a black bar (2 0.6), and a small white circle (diameter = 0.6). As is shown in Fig. 1*A*, the white fixation cross was always visible at the center of the screen against a gray background [RGB (80 80 80)] throughout a session. The black bar was randomly displayed at either the right or the left of the screen. At the beginning of each trial, the center of the bar was initially put 6.67 above and 7 to the right or the left of the fixation cross. After its appearance, the bar immediately moved toward the opposite side of the screen. As the frame-to-frame spatial offset was 0.1 , the constant and smooth speed of the bar was 10 /s. The small white circle, whose diameter was equal to the width of the bar, was flashed 6.67 above the fixation cross for one refresh frame (10 ms). When the bar crossed the center of the screen, the circle flashed at different timings (6, 4, 2, 0, 2, 4, and 6 refresh cycles of the monitor, or 60 ms to 60 ms) so that it appeared at various locations relative to the bar.

Task procedure.

Participants were seated in a dark room and viewed binocularly the screen from a distance of 60 cm, with their heads placed on a chin tray. Throughout a trial, they fixated on the white fixation cross. Then the bar appeared and moved to the opposite side, when the white circle was flashed, participants were asked to indicate its position relative to the bar (the left or right). Thus, the task was an unspeeded and two-alternative forced-choice response. In 1 s after the response, the next trial began. To avoid the expectance effect of the flashed circle, we added two perturbation conditions where the initial positions of both the small white circle and the bar were shifted by the left and right 0.5 relative to the white

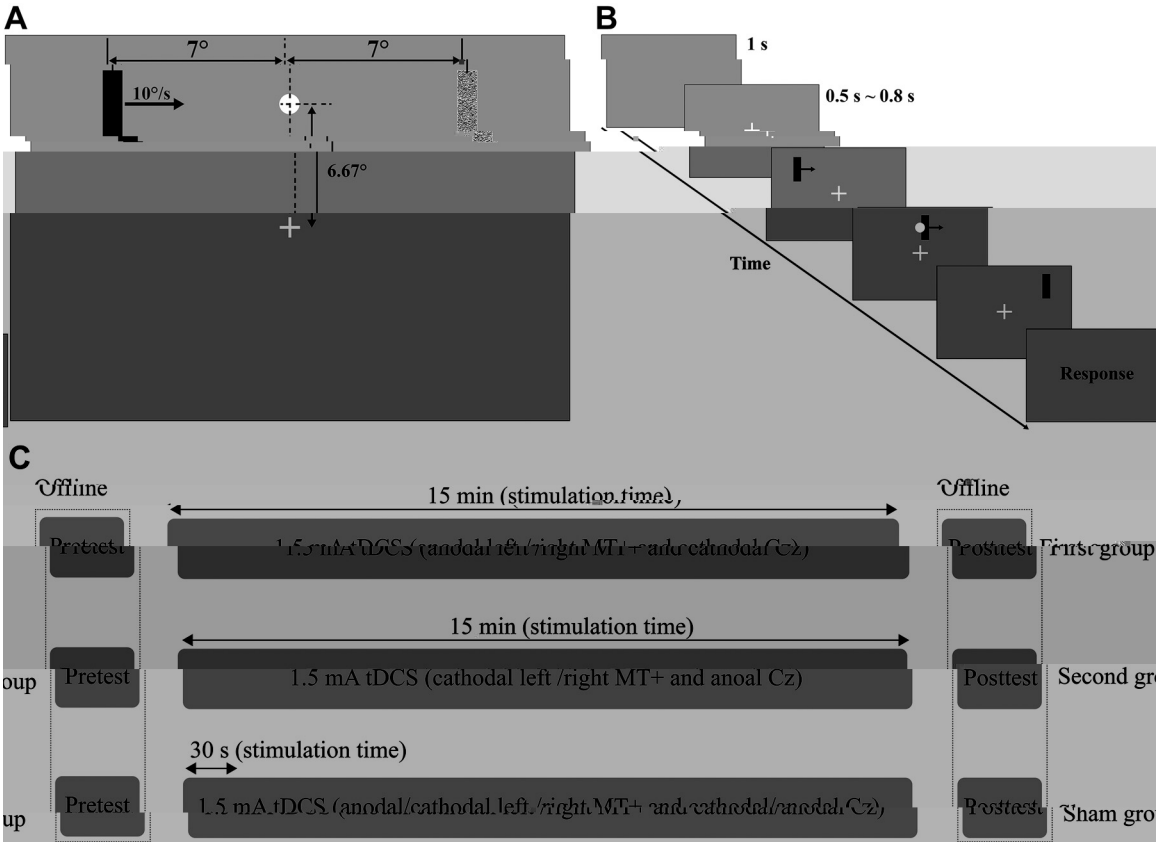

Figure 1. Depictions of stimulus displays, an example of one trail of the flash-lag task, and experimental setups for the anodal, cathodal, and sham stimulation. A: depictions of stimulus displays. Stimuli contain a white fixation cross, a black bar (2 0.6), and a small white circle (diameter = 0.6). The black bar is randomly displayed at either the right (position with a rectangle texture) or the left of the screen. B: an example of one trail of the flash-lag task. During one trial of the flash-lag task, the participant fixates on the white fixation, after 0.5–0.8 s, the black bar appears on one side of the screen and immediately moves toward the opposite side. During the movement of the bar, the small white circle is flashed above the fixation cross for one refresh frame at different timings. When the bar moves to the terminal and disappears, the participant is indicated to report the relative positions of the circle and the bar. If they perceive that the flashed circle is located on the left relative to the bar, they press the left button of a mouse; if they perceive that the flashed circle is located on the right relative to the bar, they press the right button of the mouse; if they perceive that the flashed circle completely coincides with the bar in space, they have to make an arbitrary choice. In 1 s after the response, the next trial begins. C: the experimental setups for the anodal, cathodal, and sham stimulation with different electrodes. Each group performed two sessions (pre- and posttests) of the flash-lag task under an offline condition. Between sessions, each group received the correspondent current stimulation. Cz, central parietal lobe; tDCS, transcranial direct current stimulations.

fixation cross. In addition to seven various timings of the flashed circle, we applied randomly a repetition of 21 trials for each timing. Therefore, the block from the right to the left motion consisted of 147 trials, and so did the block from the right to the left motion. Finally, a session, including the two blocks, consisted of 294 trials and lasted 15 min. Before the formal experiment, we provided a practice block of 42 trials that traversed all conditions.

Study protocol.

We applied a randomized single-blind design to assign the participants into three experiment groups (anodal vs. cathodal vs. sham). Each group performed two sessions (pre- and posttests) of the flash-lag task. Between sessions, the anodal group received the anodal stimulation. Two elastic headstraps were used to fix the anodal electrode over the left MTþ and the cathodal electrode over the Cz. After the fixation of the electrodes, the participants received the current with an intensity of 1.5 mA for 15 min; for the cathodal group, they received the same current with the cathodal electrode over the left MTþ and the anodal electrode over the Cz; for the sham group, participants received the same current for 30 s, after that the current was turned off (Fig. 1*C*). In addition, we used a tool (ROAST) to model the normal component of the electrical field (V/m) created by the montage targeting the left MTþ (see Fig. 2, *left*);381.7ree ei6.4(n)14.120.1(n89.2(thit2.1(n)y(o)19.6(g)]T)16.(r)0(a)0(t)14)0(r)21(t)20.1(iv)ss20.7(e)-

Figure 3. Effects of transcranial direct current stimulations (tDCS) over the left MTþ on the flash-lag effect (FLE) in different motion directions. A: effects of anodal (a)-tDCS. The pretest point of subjective equality (PSE) is significantly higher than the posttest PSE in the right to the left (RL) motion direction; the pretest PSE is nearly equal to the posttest PSE in the left to the right (LR) motion direction. B: effects of cathodal (c)-tDCS. The pretest PSE is significantly lower than the posttest PSE in the RL motion direction; the pretest PSE is nearly equal to the posttest PSE in the LR motion direction. C: effects of the sham tDCS. There are no significant results; the test PSEs are nearly equal. D: effects of tDCS over the left MTþ on the FLE in the RL motion direction. To avoid the individual difference and better verify the effects of tDCS on the FLE in the RL motion direction, we normalized pre- and posttests of the PSE in each group using a min-max normalization method. The normalized pre- and posttest PSEs in three types of stimulations do not significantly differ, respectively; in the anodal stimulation, the normalized pretest PSE is significantly higher than the normalized posttest PSE; in the cathodal stimulation, the normalized pretest PSE is significantly lower than the normalized posttest PSE. Hollow circles represent individual points in each group. $P < 0.01$; ns, nonsignificant.

the normalized pretest PSE was higher than the normalized posttest PSE in the anodal stimulation (t_{42} = 4.17, $P <$ 0.001, Cohen's d = 1.10), the normalized pretest PSE was lower than the normalized posttest PSE in the cathodal stimulation (t_{42} = 4.07, $P < 0.001$, Cohen's d = 1.08) (Fig. 3*D*).

To further verify the increased effect of tDCS on the FLE in the LR motion direction, we run a 2 (testing: pretest vs. posttest, within-group) 2 (stimulation: anodal vs. sham, between-group) mixed-model ANOVA with the PSE as the dependent measure (49). We observed a significant testing stimulation interaction effect ($F_{1,28}$ = 4.90, $P < 0.05$, η_p^2 = 0.15) (Fig. 4*A*). A simple effect analysis indicated that the pretest PSE was higher than the posttest PSE in the anodal stimulation (t_{28} = 3.28, $P < 0.01$, Cohen's d = 0.86), and no other significant results were found. Furthermore, we compared the discrepancy of increase effect between anodal and sham groups. The increase in PSE (posttest – pretest) was estimated via the independent sample t test (two-tailed), with the result indicating that the increased effect in the anodal group was more than that in the sham group (t_{28} = 2.21, $P < 0.05$, Cohen's d = 0.81) (Fig. 4*B*). Likewise, we further confirmed the decreased effect of tDCS on the FLE in the RL motion direction, we run a 2 (testing: pretest vs. posttest, within-group) 2 (stimulation: cathodal vs. sham, between-group) mixed-model ANOVA with the PSE as the dependent measure. We observed a significant testing stimulation interaction effect ($F_{1,28}$ = 12.22, $P < 0.01$, η_p^2 = 0.15) (Fig. 4*C*). A simple effect analysis indicated that the pretest PSE was lower than the posttest PSE in the cathodal stimulation (t_{28} = 4.79, $P < 0.001$, Cohen's d = 1.26), and no other significant results were found. Furthermore, we compared the discrepancy of the decreased effect between cathodal and sham groups. The decrease in PSE (posttest pretest) was estimated via the independent sample t test (two-tailed), with the result indicating that the decreased effect in the cathodal group was more than that in the sham group (t_{28} = 3.50, $P < 0.01$, Cohen's d = 1.28) (Fig. 4*D*).

Experiment 2: E ects of tDCS over the Right MT1 on the FLE

Participants.

A total of 45 new participants were recruited to assign into three experimental groups: anodal group (aged 19–27 yr, mean 22.0 ± 2.9 yr; 9 females; 4 left-dominated eye; all right-handedness), cathodal group (aged 19–27 yr, mean 20.0 ± 2.9 yr; 7 females; 8 left-dominated eye; all right-handedness), and sham group (aged 18–26 yr, mean 21.3 ± 2.8 yr; 9 females; 7 left-dominated eye; 1 left-handedness), whose general characteristics were the same as those in *experiment 1*.

Transcranial direct current stimulation.

tDCS parameters were the same as those in *experiment 1*, except that the left MTþ was replaced by the right MTþ .

The flash-lag task.

We used the same apparatus, stimuli, and procedure as used in *experiment 1*.

Study protocol.

The protocol was as in *experiment 1* (Fig. 1*C*), except that, for the sham group, the electrode positions on eight participants were placed over the same sites as in the anodal group, and the electrode positions on seven participants were the same sites as in the cathodal group, which makes a counterbalance

Figure 4. Increase and decrease effects of transcranial direct current stimulations (tDCS) over the left MTþ on the flash-lag effect (FLE) in the right to the left (RL) motion direction. A: increased effect of anodal (a)-tDCS. The pretest point of subjective equality (PSE) is significantly higher than the posttest PSE in the anodal group; the pretest PSE is nearly equal to the posttest PSE in the sham group. B: an comparison of the increased effect between the anodal and sham groups. The increased effect improvement is defined as (the posttest PSE the pretest PSE), and the increased effect in the anodal group is significantly higher than that in the sham group. C: decreased effect of cathodal (c)-tDCS. The pretest PSE is significantly lower than the posttest PSE in the cathodal group; the pretest PSE is nearly equal to the posttest PSE in the sham group. D: an comparison of the decreased effect between the cathodal and sham groups. The decreased effect improvement is defined as (the posttest PSE the pretest PSE), and the decreased effect in the anodal group is significantly higher than that in the sham group. Hollow circles represent individual points in each group. $P < 0.05$, $P < 0.01$; ns, nonsignificant.

on the electrode position number in two sham groups in two experiments. In addition, the current electrical field (V/m) created by the montage targeting the right MTþ is shown in Fig. 2, *right*.

Data processing and analysis.

We used the same data processing and analysis as in *experiment 1*.

Results.

To estimate the effects of tDCS on the right MTþ on the FLE in different motion directions, we performed a 2 (testing: pretest vs. posttest) 2 [motion direction: the right to the left (RL) versus the left to the right (LR)] repeated-measures ANOVA with the PSE as the dependent measure in anodal, cathodal, and sham groups, respectively (see Supplemental Material). For the anodal group, we observed a significant main effect of testing ($F_{1,14} = 5.39$, $P < 0.05$, $\eta_p^2 = 0.28$) and testing motion direction interaction effect ($F_{1,14} = 7.77$, $P < 0.05$, $\eta_p^2 = 0.36$) (Fig. 4*A*). A simple interaction analysis indicated that the posttest PSE was lower than the pretest PSE in the LR motion direction ($t_{14} = 5.30$, $P < 0.01$, Cohen's $d = 0.54$) (Fig. 5*A*). For the cathodal group, we observed a significant main effect of testing ($F_{1,14} = 8.61$, $P < 0.05$, $\eta_p^2 = 0.38$) and testing motion direction interaction effect ($F_{1,14} = 14.11$, $P < 0.01$, $\eta_p^2 = 0.50$) (Fig. 5*B*). A simple interaction analysis indicated that the pretest PSE was lower than the posttest PSE in the LR motion direction ($t_{14} = 5.12$, $P < 0.01$, Cohen's $d = 0.81$) (Fig. 5*B*). For the sham group, no other significant results were found (Fig. 5*C*). For three groups, the JNDs did not significantly differ between different testings and motion directions (see Supplemental Fig. S2).

After the normalization of pre- and posttest PSEs in the LR motion direction, we run a 2 (testing: pretest vs. posttest) 2 (stimulation: anodal vs. cathodal versus sham) repeated-measures ANOVA with the normalized PSE as the dependent measure. We observed a significant testing stimulation interaction effect ($F_{2,42} = 11.00$, $P < 0.01$, $\eta_p^2 = 0.34$) (Fig. 5*D*). A simple interaction analysis (Bonferroni correction) indicated that the normalized pretest PSE was higher than the normalized posttest PSE in the anodal stimulation ($t_{42} = 2.16$, $P < 0.05$, Cohen's $d = 0.57$), the normalized pretest PSE was lower than the normalized posttest PSE in the cathodal stimulation ($t_{42} = 4.37$, $P < 0.001$, Cohen's $d = 1.15$), with no other significant results found (Fig. 5*D*).

To further verify the increased effect of tDCS on the FLE in the RL motion direction, we run a 2 (testing: pretest vs. posttest, within-group) 2 (stimulation: anodal vs. sham, between-group) mixed-model ANOVA with the PSE as the dependent measure (49). We observed a marginally significant testing stimulation interaction effect ($F_{1,28} = 3.47$, $P = 0.073$, $\eta_p^2 = 0.11$) (Fig. 6*A*). A simple effect analysis indicated that the pretest PSE was higher than the posttest PSE in the anodal stimulation ($t_{28} = 2.61$, $P = 0.015 < 0.05$, Cohen's $d = 0.69$), and no other significant results were found. Furthermore, we compared the discrepancy of the increased effect between anodal and sham groups. The increase in PSE (posttest pretest) was estimated via the independent sample t test (two-tailed), with the result indicating that the increased effect in the anodal group was marginally more than that in the sham group ($t_{28} = 1.86$, $P = 0.073$, Cohen's $d = 0.68$) (Fig. 6*B*). Likewise, we further confirmed the decreased effect of tDCS on the FLE in the LR motion direction, we run a 2 (testing: pretest vs. posttest, within-group) 2 (stimulation: cathodal vs. sham, between-

group) mixed-model ANOVA with the PSE as the dependent measure. We observed a significant testing stimulation interaction effect ($F_{1,28} = 6.68$, $P < 0.05$, $\eta_p^2 = 0.20$) (Fig. 6*C*). A

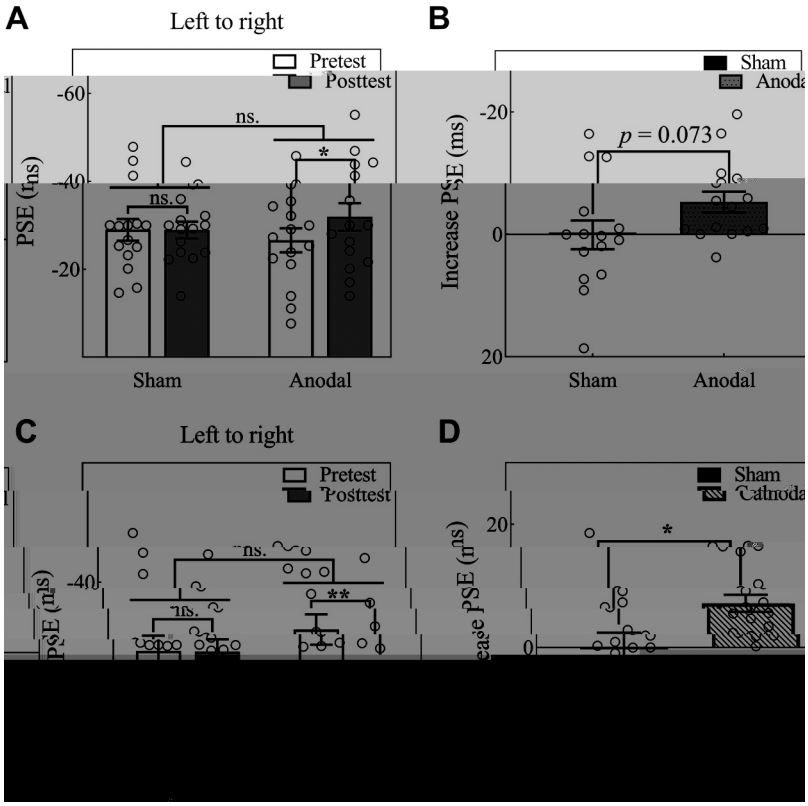

Figure 6. Increase and decrease effects of transcranial direct current stimulations (tDCS) over the right MTþ on the flash-lag effect (FLE) in the left to the right (LR) motion direction. A: increased effect of anodal (a)-tDCS. The pretest point of subjective equality (PSE) is significantly higher than the posttest PSE in the anodal group; the pretest PSE is nearly equal to the posttest PSE in the sham group. B: an comparison of the increased effect between the anodal and sham groups. The increased effect improvement is defined as (the posttest PSE the pretest PSE), and the increased effect in the anodal group is marginally higher than that in the sham group. C: the decreased effect of cathodal (c)-tDCS. The pretest PSE is significantly lower than the posttest PSE in the cathodal group; the pretest PSE is nearly equal to the posttest PSE in the sham group. D: an comparison of the decreased effect between the cathodal and sham groups. The decreased effect improvement is defined as (the posttest PSE the pretest PSE), and the decreased effect in the anodal group is significantly higher than that in the sham group. Hollow circles represent individual points in each group. $P < 0.05$, $P < 0.01$, ns, nonsignificant.

direction decreased (Fig. 5, *B* and *D* and Fig. 6, *C* and *D*). A similar explanation for this result is that the cathodal stimulation might decrease the cortical excitability in MTþ (32, 33, 35), which might shift the perceptual localization of the moving bar away from the side of the brain stimulated when a flash appears. Since c-tDCS also affected the PSE but not the JND, it may also introduce a perceptual decision bias in MTþ (50). Furthermore, c-tDCS on unilateral MTþ possibly decreased the total activity of a subpopulation of MTþ neurons (tuned to target direction), thereby leading to a decrease in the perceived speed of the moving bar toward the side stimulated, which reduces the magnitude of the FLE. Alternatively, c-tDCS on unilateral MTþ might impose top-down feedback to V1, which indirectly influences the "perceived position" of the moving bar away from the side stimulated.

Although our results clearly showed that the current stimulation of MTþ modulates the magnitude of the FLE, the identification of the mechanisms through which tDCS affects visual motion perception still requires further discussion. Indeed, tDCS can enhance and decrease cortical excitability in MTþ (30, 33, 35, 38). Interestingly, the modulation mechanisms of tDCS on motion perception may be different as visual motion task changes (33, 37). In our study, although the moving bar is easy to detect, a-tDCS, by increasing the probability of the firing rate, may activate more neurons tuned to the moving bar (56, 57). In particular, even those that originally do not reach the activation in the absence of stimulation may excite as a result of a-tDCS. Hence, a-tDCS might result in temporarily more neurons being activated to represent the moving bar, thereby overestimating the perceived speed of the moving bar than that in no stimulation (53, 58). Conversely, c-tDCS may depress those neurons tuning to the moving bar and attenuate the moving bar representation, thereby underestimating the perceived speed of the moving bar (52, 58). Alternatively, tDCS may modulate the top-down feedback from MTþ to V1, which biases the position coding in V1 and then induces perceived position shift due to motion perception (4, 10, 59, 60). One possibility is that the change of perceived position shift in V1 is attributable to the strength of motion processing in MTþ due to tDCS (4, 59); the other possibility is that the connectivity efficacy from MTþ to V1 might be mediated by tDCS, which causes the change of perceived position shift (3, 9).

In addition, our findings have implications for spatial mechanisms for the FLE, although the present study was not designed to falsify one of the various mechanism interpretations. Spatial mechanisms explain the FLE as a predictive forward shift of the moving object, potentially compensating for the transmission delays of the visual signal from the eye to the visual cortex (4, 6, 8). Indeed, predictable motion preactivates the future positions of moving objects and attenuated the neural response to objects moving into a predictive region (6, 61, 62). Thus, perceptual position shifts are thought to be the result of an interaction of lateral inhibition and excitation in retinotopic maps and/or feedback from the higher areas. Furthermore, modifying neural activity in MTþ might directly interfere with perceived motion and/or feedback signals, which would usually change a misalignment in the motion direction.

Also, our results did not well distinguish the pre- and post-flashed stimulus-dependent temporal processings in the FLE. Interestingly, tDCS did only affect the PSE but not the JND, indicating that tDCS might modulate the perceptual

decision processing in the FLE, which indicates that early visual signals evoked by the moving bar are necessary for or correlated with the later decision processing (63). Although motion extrapolation or postdiction account did not separately interpret the current results, the modulation effect of tDCS on the FLE suggests that the later decision processing in MTþ likely imposes the top-down feedback to V1, affecting the perceived position of the moving bar. The agreement reconciles with one statement that the primary visual regions contralateral to the poststimulus movement are critical for the FLE (64). Therefore, the present findings suggest that tDCS might modulate the postflash decision processing in the FLE.

The FLE points out the significant difficulties that the visual system has while trying to correctly pinpoint the physical locations of moving objects. But the visual system attempts to correct the positional error by some neural mechanisms, which made psychophysical outcomes on the FLE multifaceted and complicated. Therefore, the modulation effects of tDCS over MTþ on the FLE require

24. Thompson B, Deblieck C, Wu A, Iacoboni M, Liu Z. Brain stimulation psychophysical and rTMS evidence for the presence of motion opponency in human V5. Brain Stimul 9: 876–881, 2016. doi:10.1016/j.brs.2016.05.012.
25. Zinchenko A, Brunner S, Chen L, Shi Z, Paul C, Taylor J, Müller HJ. V5/MT þ modulates spatio-temporal integration differently across and within hemifields: causal evidence from TMS. Neuropsychologia 161: 107995, 2021. doi:10.1016/j.neuropsychologia.2021.107995.
26. Thakral PP, Slotnick SD. Disruption of MT impairs motion processing. Neurosci Lett 490: 226–230, 2011. doi:10.1016/j.neulet.2010.12.057.
27. Akin B, Ozdem C, Eroglu S, Keskin DT, Fang F, Doerschner K, Kersten D, Boyaci H. Attention modulates neuronal correlates of interhemispheric integration and global motion perception. J Vis 14: 30, 2014. doi:10.1167/14.12.30.
28. Amano K, Wandell BA, Dumoulin SO. Visual field maps, population receptive field sizes, and visual field coverage in the human MTþ complex. J Neurophysiol 102: 2704–2718, 2009. doi:10.1152/jn.00102.2009.
29. Huk AC, Dougherty RF, Heeger DJ. Retinotopy and functional subdivision of human areas MT and MST. J Neurosci 22: 7195–7205, 2002. doi:10.1523/JNEUROSCI.22-16-07195.2002.
30. McGraw PV, Walsh V, Barrett BT. Motion-sensitive neurones in V5/MT modulate perceived spatial position. Curr Biol 14: 1090–1093, 2004. doi:10.1016/j.cub.2004.06.028.
31. Whitney D, Ellison A, Rice NJ, Arnold D, Goodale M, Walsh V, Milner D. Visually guided reaching depends on motion area MTþ. Cereb Cortex 17: 2644–2649, 2007. doi:10.1093/cercor/bhl172.
32. Antal A, Nitsche MA, Paulus W. Transcranial direct current stimulation and the visual cortex. Brain Res Bull 68: 459–463, 2006. doi:10.1016/j.brainresbull.2005.10.006.
33. Battaglini L, Noventa S, Casco C. Anodal and cathodal electrical stimulation over V5 improves motion perception by signal enhancement and noise reduction. Brain Stimul 10: 773–779, 2017. doi:10.1016/j.brs.2017.04.128.
34. Bestmann S, de Berker AO, Bonaiuto J. Understanding the behavioural consequences of noninvasive brain stimulation. Trends Cogn Sci 19: 13–20, 2015. doi:10.1016/j.tics.2014.10.003.
35. Antal A, Nitsche MA, Kruse W, Kincses TZ, Hoffmann KP, Paulus W. Direct current stimulation over V5 enhances visuomotor coordination by improving motion perception in humans. J Cogn Neurosci 16: 521–527, 2004. doi:10.1162/089892904323057263.
36. Antal A, Nitsche MA, Kincses TZ, Kruse W, Hoffmann KP, Paulus W. Facilitation of visuo-motor learning by transcranial direct current stimulation of the motor and extrastriate visual areas in humans. Eur J Neurosci 19: 2888–2892, 2004. doi:10.1111/j.1460-9568.2004.03367.x.
37. Miniussi C, Harris JA, Ruzzoli M. Modelling non-invasive brain stimulation in cognitive neuroscience. Neurosci Biobehav Rev 37: 1702–1712, 2013. doi:10.1016/j.neubiorev.2013.06.014.
38. Antal A, Varga ET, Nitsche MA, Chadaide Z, Paulus W, Kovács G, Vidnyánszky Z. Direct current stimulation over MTþ/V5 modulates motion aftereffect in humans. Neuroreport 15: 2491–2494, 2004. doi:10.1097/00001756-200411150-00012.
39. Pelli DG. The VideoToolbox software for visual psychophysics: transforming numbers into movies. Spat Vis 10: 437–442, 1997.
40. Brainard DH. The psychophysics toolbox. Spat Vis 10: 433–436, 1997. doi:10.1163/156856897X00357.
41. Huang Y, Datta A, Bikson M, Parra LC. ROAST: an open-source, fully-automated, realistic volumetric-approach-based simulator for TES. Annu Int Conf IEEE Eng Med Biol Soc 2018: 3072–3075, 2018. doi:10.1109/EMBC.2018.8513086.[30441043]
42. Huang Y, Datta A, Bikson M, Parra LC. Realistic volumetric-approach to simulate transcranial electric stimulation—ROAST—a fully automated open-source pipeline. J Neural Eng 16: 056006, 2019. doi:10.1088/1741-2552/ab208d.
43. Liu Y, Yang J, Yu Y, Yu Y, Wang W, Li H, Takahashi S, Ejima Y, Wu Q, Wu J. A new method for haptic shape discriminability detection. Appl Sci 11: 1–19, 2021. doi:10.3390/app11157049.
44. Wang W, Yang J, Yu Y, Wu Q, Yu J, Takahashi S, Ejima Y, Wu J. Tactile angle discriminability improvement: Roles of training time intervals and different types of training tasks. J Neurophysiol 122: 1918–1927, 2019. doi:10.1152/jn.00161.2019.
45. Wang W, Yang J, Yu Y, Li H, Liu Y, Yu Y, Yu J, Tang X, Yang J, Takahashi S, Ejima Y, Wu J. Tactile angle discriminability improvement: contributions of working memory training and continuous attended sensory input. J Neurophysiol 127: 1398–1406, 2022. doi:10.1152/jn.00529.2021.
46. Wang W, Yang J, Yu Y, Wu Q, Takahashi S, Ejima Y, Wu J. Tactile semiautomatic passive-finger angle stimulator (TSPAS). J Vis Exp 161: e61218, 2020. doi:10.3791/61218.
47. Bao H-W-S. bruceR: broadly useful convenient and efficient R functions (Online). https://cran.r-project.org/package=bruceR [2022 Jul 3].
48. Jain A, Nandakumar K, Ross A. Score normalization in multimodal biometric systems. Pattern Recognit 38: 2270–2285, 2005. doi:10.1016/j.patcog.2005.01.012.
49. Nieuwenhuis S, Forstmann BU, Wagenmakers EJ. Erroneous analyses of interactions in neuroscience: a problem of significance. Nat Neurosci 14: 1105–1107, 2011. doi:10.1038/nn.2886.
50. Battaglini L. Effect of repetitive transcranial magnetic stimulation on